2010

Low-Cost Obstacle Detection Sensor Array for Unmanned Agricultural Vehicles

Santosh Pitla
University of Nebraska-Lincoln, spitla2@unl.edu

Joe D. Luck
University of Nebraska-Lincoln, jluck2@unl.edu

Scott A. Shearer
University of Kentucky, Scott.A.Shearer@uky.edu

2950 Niles Road, St. Joseph, MI 49085-9659, USA
269.429.0300 fax 269.429.3852 hq@asabe.org www.asabe.org

An ASABE Meeting Presentation

Paper Number: 1008702

Low-Cost Obstacle Detection Sensor Array for Unmanned Agricultural Vehicles

S.K.Pitla, Engineer Associate

Biosystems and Agricultural Engineering, University of Kentucky, Lexington, KY40546, santosh.pitla@bae.uky.edu

J.D.Luck, Engineer Associate

Biosystems and Agricultural Engineering, University of Kentucky, Lexington, KY40546, luck.joe@bae.uky.edu

S.A.Shearer, Professor

Biosystems and Agricultural Engineering, University of Kentucky, Lexington, KY40546, Scott.A.Shearer@ uky.edu

Written for presentation at the
2010 ASABE Annual International Meeting
Sponsored by ASABE
David L. Lawrence Convention Center
Pittsburgh, Pennsylvania
June 20 – June 23, 2010

Abstract. *Mobile robots deployed for agricultural applications must operate in harsh environments where they encounter a variety of both moveable and immovable obstacles. Typically, robots utilize vision sensors to learn about the environment in which they are working. In this study, a low-cost infra-red (IR) sensor array was developed to act as an obstacle detection aid for an unmanned agricultural vehicle (UAgV). The IR sensor array developed consists of six IR sensors mounted on two orthogonal steel plates. The array of sensors was continuously oscillated about the yaw-axis to traverse a 200^0 field of view in front of the UAgV. Three identical cylindrical barrels were used as obstacles to evaluate the response of the sensor array in four scenarios for initial testing. In all the four scenarios, the IR sensor array was able to detect the barrels placed within the sensing range (1 m to 5 m) and the field of view (200^0).*

Keywords. *Unmanned agricultural vehicles, IR sensors, mobile robots, autonomous vehicles*

Introduction

With the recent developments in the area of automation technology, the deployment of autonomous machines for agricultural tasks is on the horizon. Safety and liability forms the major areas of concern any time the notion of implementing unmanned agricultural vehicles (UAgVs) is addressed. The absence of a supervisor/operator on the machine mandates the UAgV to be intelligent and responsive to the environment. Sensors act as gateway to learn about the environment in which the UAgV is working. Typically ultrasonic, IR and laser sensors have been used by researchers for obstacle identification and low cost autonomous guidance. The range information obtained from these sensors is utilized to achieve localization and obstacle free navigation. The accuracy, range and field of view of the sensors are of paramount importance to interpret the environment that the UAgV is experiencing.

Different sensors have their own advantages and disadvantages and one of the main criteria which determine the usability of sensors in practical systems is the cost of the sensor. Expensive sensors provide accurate ranging information but they may not always be suitable for mobile applications because of their demand for high computation power and increased data processing time. The environment in which the UAgVs work is continuously changing and response time of the sensors is crucial when it has to react to the obstacles. Low cost sensors, on the other hand do not provide all the necessary information even though the processing times and computation overhead is low. CCD cameras, ultrasonic sensors, scanning lasers (including 2D and 3D) and millimeter wave radar are some of the technologies that researchers have used to detect obstacles (Gray 2002). Stereo vision utilizes CCD cameras and operates in principle similar to a human eye that requires light to identify the objects. This technology offers some disadvantages for the UAgVs especially when the agricultural tasks are performed during early mornings and nights. Wei et al (2005) used a binocular stereo camera to detect obstacles and concluded that with increase in the distance range of obstacle from the autonomous vehicle, the accuracy of the system decreased. Although stereo vision identifies obstacles efficiently, the excessive computation required to obtain useful information from stereo vision makes it an unfavorable choice for incorporating them in real-time obstacle detection systems. Ultrasonic sensors are very popular among researchers as they are relatively cheap and simple to use. Obstacle avoidance algorithms were developed by Bronstein (1998) with ultrasonic sensors as the obstacle detection device. They were used on mobile robots and agricultural vehicles for localization, navigation and obstacle detection. Short range of sight and their requirement to be perpendicular to the target surface for obtaining accurate measurements limits the use of ultrasonic sensors as obstacle detection devices in agricultural environments. Range of sensors becomes especially critical in agricultural applications where the tractors travel at speeds of 5 to 8 mph. Scanning laser is another sensing technology which gained popularity over stereo vision and ultrasonic sensors because of its ability to provide accurate ranging measurements. Matthies et al (2003) demonstrated obstacle detection and avoidance in dense tall grass using a SICK ladar. Although the scanning lasers have good resolution and accuracy, it suffers from some drawbacks. Scanning lasers are susceptible to dust and rain and errors in ranging measurements can be induced in the field. 2-D scanning lasers are expensive and the cost to upgrade to 3-D scanning lasers is very steep. The cost of scanning lasers sometimes can easily exceed the cost of autonomous machine itself. This study aims to develop a sensor array using low-cost IR sensors which can be utilized as an obstacle detection aid for a UAgV. The construction details and the response of sensor array to obstacles under different conditions are discussed in the following sections.

Objectives

The main objectives of this study were

- To develop a low cost IR sensor array for detecting obstacles
- To evaluate the response of the IR sensor array in detecting obstacles in four scenarios

Materials and Methods

The low cost IR sensor utilized for this project was SHARP GP2Y0A700K (SHARP CORPORATION) which had a sensing range of 1m to 5.5 m. The sensor was calibrated in the laboratory using a cardboard target. The sensor was calibrated by placing the sensor at distances of 1m to 4 m in steps of 0.5 m from the target. A total of six IR sensors were used to construct the sensor array that scans the area in front of the robot for obstacles.

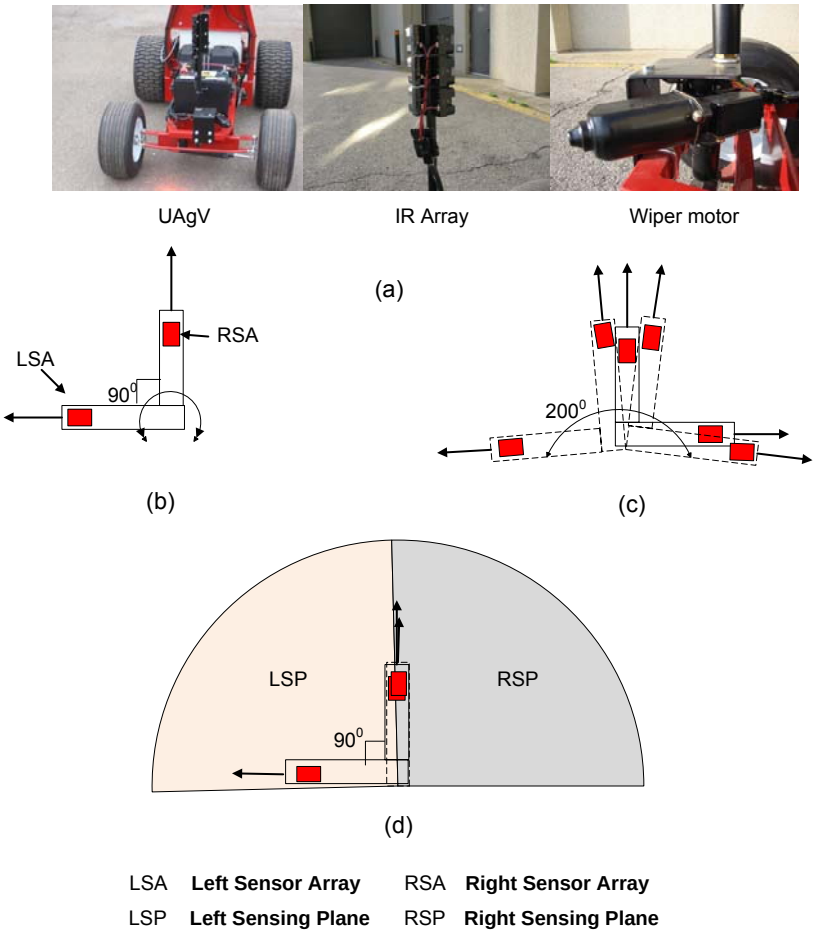

Figure 1. (a) UAgV and IR sensor array (b) Right sensor array (RSA) and Left sensor array (LSA) (c) Field of view of the sensor array (d) Sensing planes (LSP, RSP)

The IR sensor array consists of two orthogonal steel plates (fig.1b) with three IR sensors on each plate. The three IR sensors on each steel plate allowed the UAgV (fig.1a) to detect obstacles at different heights. An oscillating wiper motor (fig.1a) with 110^0 rotation capability was used to rotate the sensor array about the yaw axis. A separation of 90^0 between the steel plates and the ability of the oscillating motor to rotate 110^0 allowed the sensor array to achieve a field of view of 200^0 (fig.1c). The scanning rate of the IR sensor array was found to be 200^0/s. The right sensor array (RSA) and the left sensor array (LSA) can sense obstacles that the UAgV might encounter in the right sensing plane (RSP) and the left sensing plane (LSP) respectively (fig.1d). Any object/obstacle in line with the UAgV's path can be assumed to be located at the intersection area of LSP and RSP where, both LSA and RSA will be able to detect the obstacle alternately due to the oscillation of the IR sensor array. Typically, redundant information about obstacles is desirable and the current design provides data from both LSA and RSA about the obstacle's proximity when the UAgV is heading towards an obstacle. Thus, the IR sensor array improves the fail-safe nature of the UAgV because when the RSA fails to detect the obstacle the LSA should be able detect it.

To determine the response of the sensor array to obstacles, four scenarios were created using three identical cylindrical barrels. A 12-bit A/D card was used for digitizing the signals obtained from the six IR sensors of the sensor array and data was collected at a rate of 10 Hz. In scenario I (fig.2a) the barrel was placed in the LSP at distances of 1, 2, 3 and 4 m to evaluate the sensing abilities of the three IR sensors (L1, L2, and L3) of the LSA. In scenario II (fig.2b), the barrel was placed in the RSP to test IR sensors (R1, R2, R3) of the RSA. Scenario III (fig.2c) was created to place an obstacle in the intersection area of the LSP and RSP where the barrel was placed straight ahead in front of the UAgV. In this case, both LSA and RSA will be able to detect the barrel. In scenario IV (fig. 2d), all the three barrels were placed along an arc of radius X within the sensing range of the infrared sensors. This scenario was created to evaluate the response of the LSA and RSA to obstacles in the total field of view (200^0) of the IR sensor array.

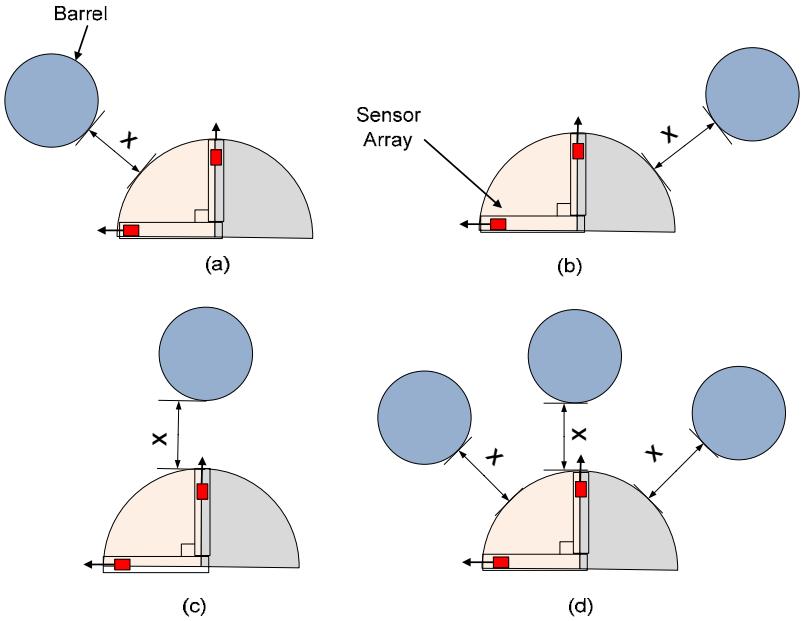

Figure 2. Obstacle Setup, X = 1, 2, 3, 4

Results and Discussion

The calibration curve obtained for the sensor was an exponential curve (fig. 3). The range of voltage output of the sensor is approximately 0.5 to 3 V for a sensing distance range of 1 to 4 m. With the increase in distance of the obstacle the voltage decreased exponentially. Thus, within the sensing range of the sensor, high magnitude output voltages from the sensor corresponds to closer objects and low output voltages corresponds to farther objects.

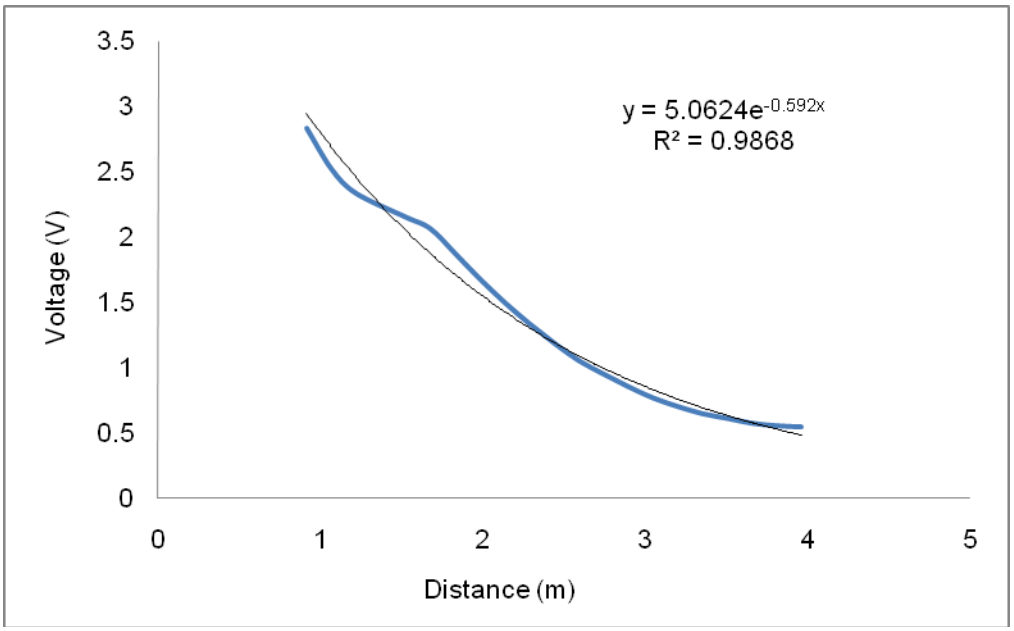

Figure 3. Calibration curve of the Infra-red sensor

For all scenarios, data from the sensor array was collected for approximately 60 s at multiple distances of X (1, 2, 3 and 4 m). The distance output obtained by LSA (L1, L2 and L3) in scenario I for the first 5 s is plotted and presented in figure 4. The LSA was able to detect the barrel placed in the LSP five times in the first 5 s. The detection of the barrels can be confirmed by observing the patterns of the data obtained in figure 4 for X = 1 m. This was intuitive as the IR sensor array was oscillating with a time period of two seconds and the barrel was detected twice in one complete oscillation of the LSA (to and fro motion).

Further visual inspection of the distance output plot revealed the occurrence of some unknown data points with a magnitude of 3.5 to 4.5 m between the patterns of barrels in figure 4 for X= 1 m. The undesirable data could be a result of experimental error. The LSA must have detected some unknown objects present within its sensing range. With an increase in the distance X, LSA was still sensing the obstacles within the sensing range (1 to 5 m), but no specific pattern was observed. There was a reduction in the number of data points corresponding to the detection of the obstacle. Fewer data points below 4.5 m were observed in the distance plot for X=2 m when compared to the distance plot for X = 1 m (fig.4)

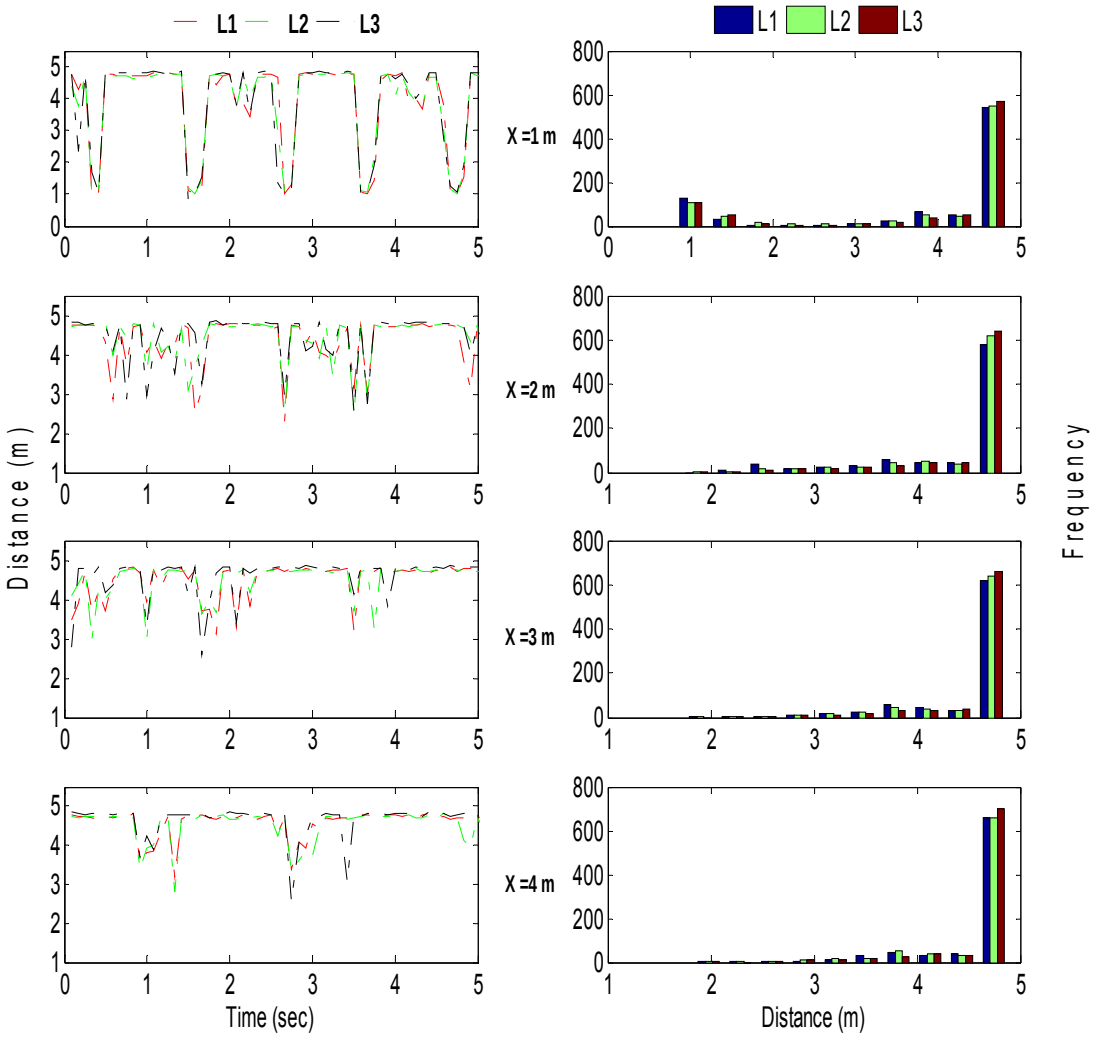

Figure 4. Distance output plot (left) and frequency distribution plot (right) in scenario 1 for X =1, 2, 3 and 4 m of the LSA

The increase distance X from 1 m to 4 m caused fewer data points to be recorded by the LSA (fig. 4). The reduction in the number of data points recorded by the sensors could be attributed to the diminishing angular resolution of the oscillating IR sensor array with an increase in the distance of the obstacle. As the obstacle moves away from the sensor fewer IR rays strike the obstacle resulting in fewer reflections returning to the sensor. Hence, the number of data points corresponding to the detection of obstacles is higher for closer objects than for farther objects. In further discussion of the results in following sections, the terms obstacle data points (ODP) and no-obstacle data points (NODP) will be used which refer to the data points obtained as a result of detecting the obstacles and not detecting any obstacles respectively. A threshold distance of 4.5 m was considered for all the scenarios. All the data points with a magnitude of less than or equal to 4.5 m will be considered as ODP and the remaining data points with a magnitude greater than 4.5 m will be treated as NODP.

To quantify the effect of distance on the sensing ability of the IR sensor array, a frequency distribution of data obtained from the LSA at distances X = 1 m to 4 m are plotted (fig.4). At X = 1 m the frequency distribution of the data obtained by L1, L2 and L3 revealed that the frequency of data was high at distances above 4.5 m. This was expected because, during data collection in scenario I, the sensors were typically detecting nothing except for the barrel placed in the LSP. The next frequency peak was observed at 1 m distance which corresponds to the presence of the barrel at 1 m in the LSP. As X increased from 1 to 4 m, the frequency bars were observed to be spread across the range of distances indicating the presence of obstacle data points less than 4.5 m. Ideally, frequency peaks should be observed at each distance of 1, 2, 3 and 4 m where barrels were placed but that was not the case. Frequency peaks were observed only at a distance of 1 m and can be observed in the frequency plot for X = 1 m. Better spatial resolution of the IR sensor array at closer target distances can be attributed to the higher frequency of data at closer distances to the obstacle.

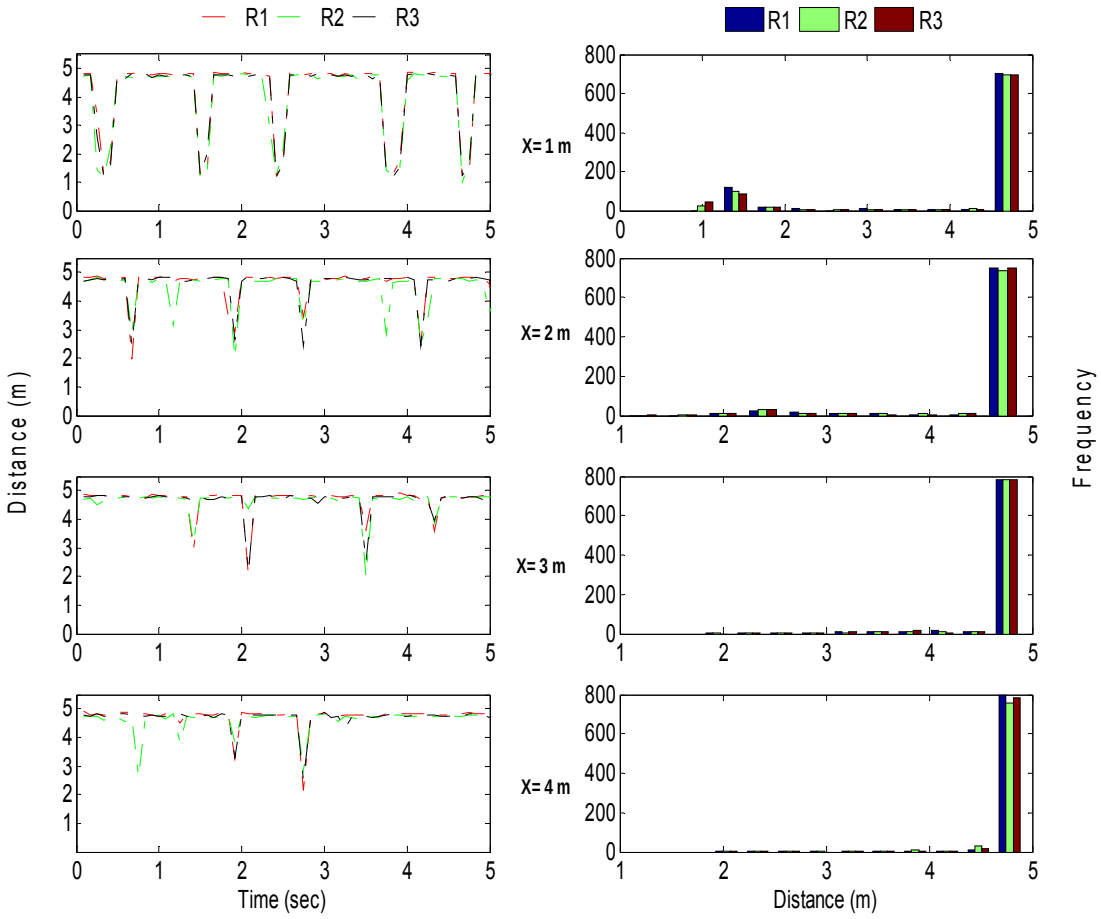

Figure 5. Distance output plot (left) and frequency distribution plot (right) in scenario II for X =1, 2, 3 and 4 m of the RSA

The barrel placed in the RSP of the sensor array in scenario 2 was detected by (R1, R2 and R3) of the RSA. The distance plot for X =1 m (fig.5) indicated that the RSA generated a pattern which is representative of presence of a barrel in the RSP and the pattern was replicated five times in the first 5 s. The data recorded by the RSA had no unwanted data in between the barrel patterns indicating that RSA was not detecting any unknown objects. Similar to scenario I, as X

increased from 1 to 4 m, the number of ODPs recorded reduced which was indicative of a reduction in sensor resolution at higher distances (fig.5). For X =1 m, the frequency distribution plot (fig.5) depicts the occurrence of the frequency peaks above 4.5 m representing NODPs and the subsequent frequency peaks between 1 and 2 m indicating the presence of the barrel near 1 m. As X increased, the no-obstacle data point frequency peaked which indicated the increase of NODPs.

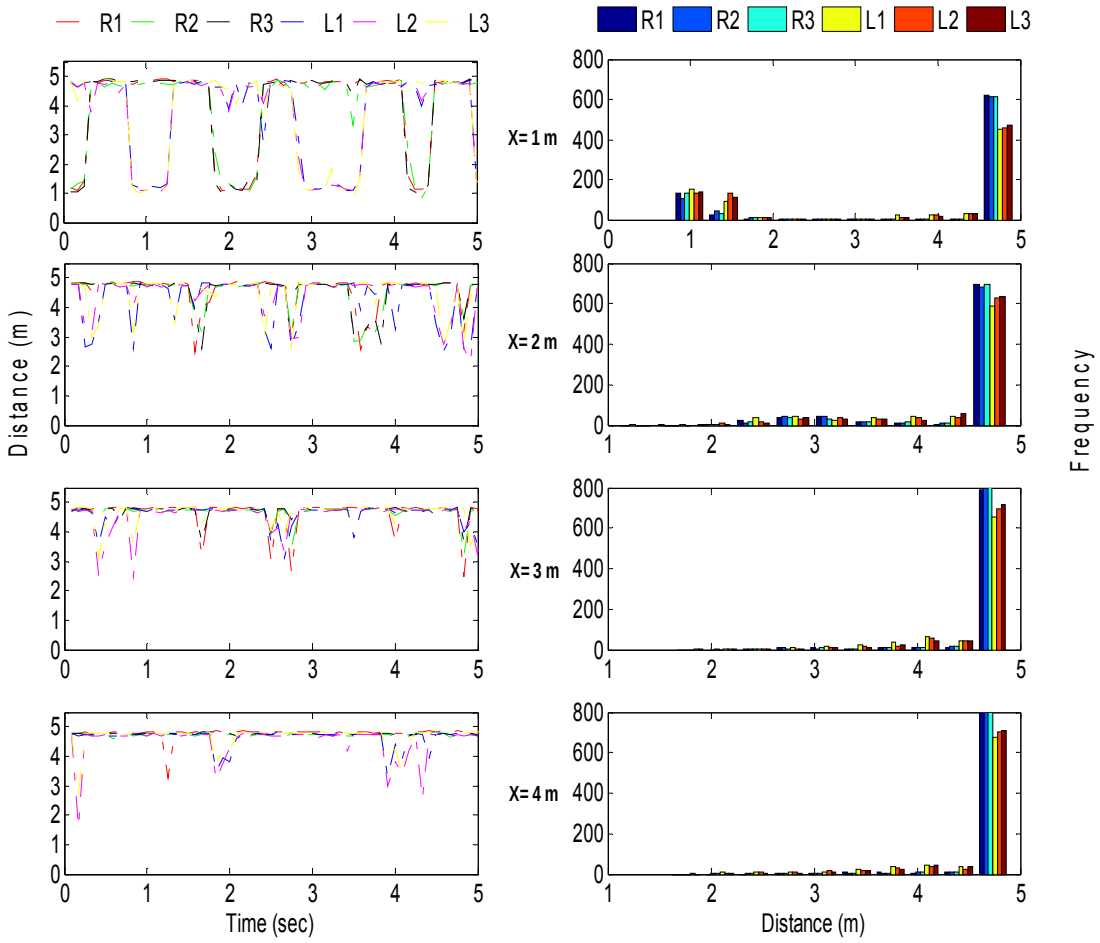

Figure 6. Distance output plot (left) and frequency distribution plot (right) in scenario III for X =1, 2, 3 and 4 m of the RSA and LSA

In scenario III, the barrel was detected by both the LSA and RSA. The distance plot for the first 5 s at X=1 m (fig.6) reveals that R1, R2, R3 and L1, L2, L3 created the barrel patterns. For X = 1 m, the frequency distribution plot (fig.6) had frequency peaks at distances greater than 4.5 m and closer to 1 m. These frequency peaks indicated the number of NODPs and the number of ODPs recorded by both the LSA and RSA. Similar to scenario I and scenario II, as the distance X increased, fewer ODPs were recorded.

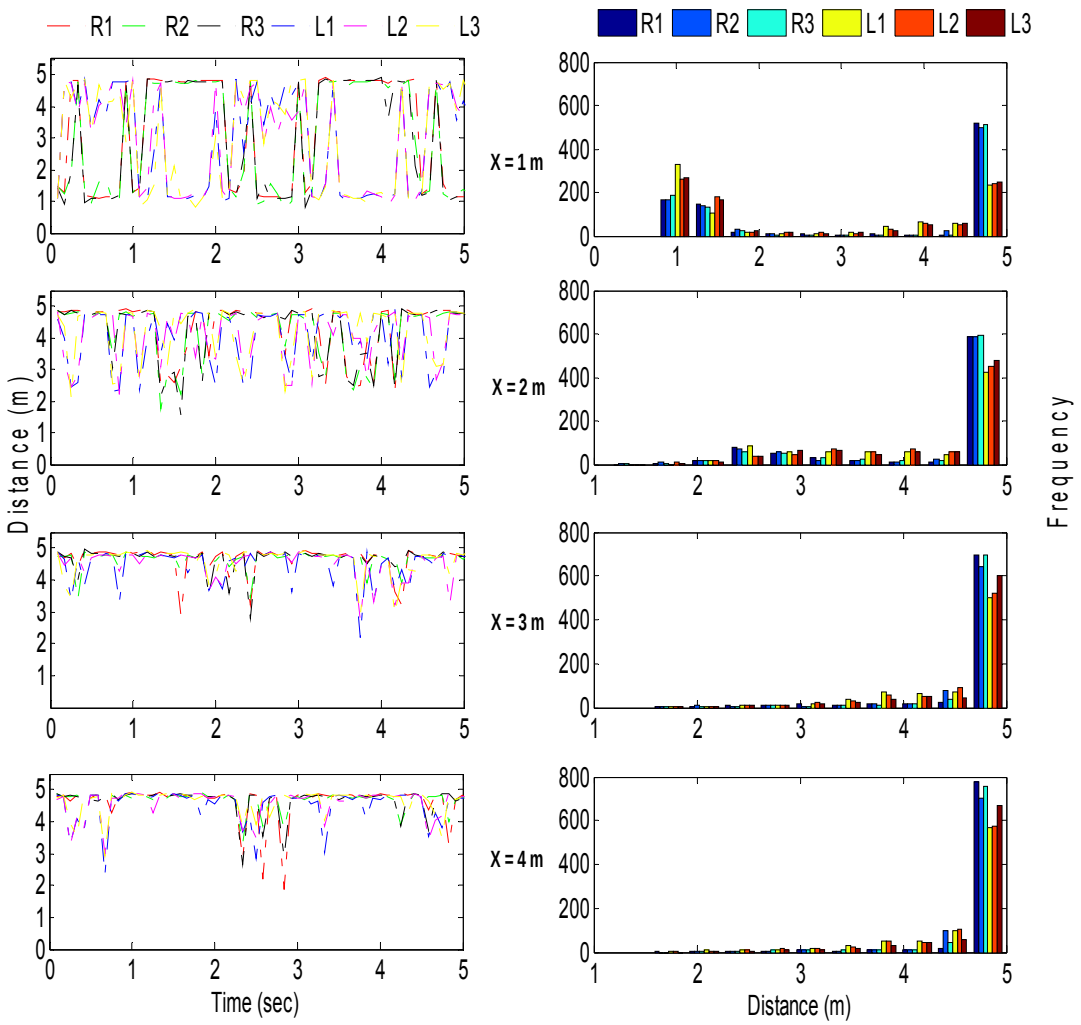

Figure 7. Distance output plot (left) and frequency distribution plot (right) in scenario IV for X =1, 2, 3 and 4 m of the RSA and LSA

Scenario IV had three barrels placed in the LSP, RSP and in the intersection area of LSP and RSP. The distance output plot at X= 1 m (fig.7) provides patterns corresponding to the barrels placed at 1 m distance. The frequency distribution plot indicates frequency peaks at distances above 4.5 m which corresponds to the NODPs and frequency peaks between 1 and 2 m representing ODPs. Since three barrels are sensed by the sensor array, the number of ODPs recorded in scenario IV was relatively higher than the number of ODPs recorded in other scenarios. As X increased the sensor resolution was reduced and fewer obstacle data points were recorded. An increase in the frequency of NODPs with increased X confirms the reduction of ODPs (fig.7).

To summarize the effect of increase in obstacle distance X on the response of IR sensor array, for all scenarios, the ratio of number of obstacle data points recorded to total number of data points recorded for each run was computed to obtain the percentage of obstacle data points obtained at each barrel distance of X = 1, 2, 3 and 4 m.

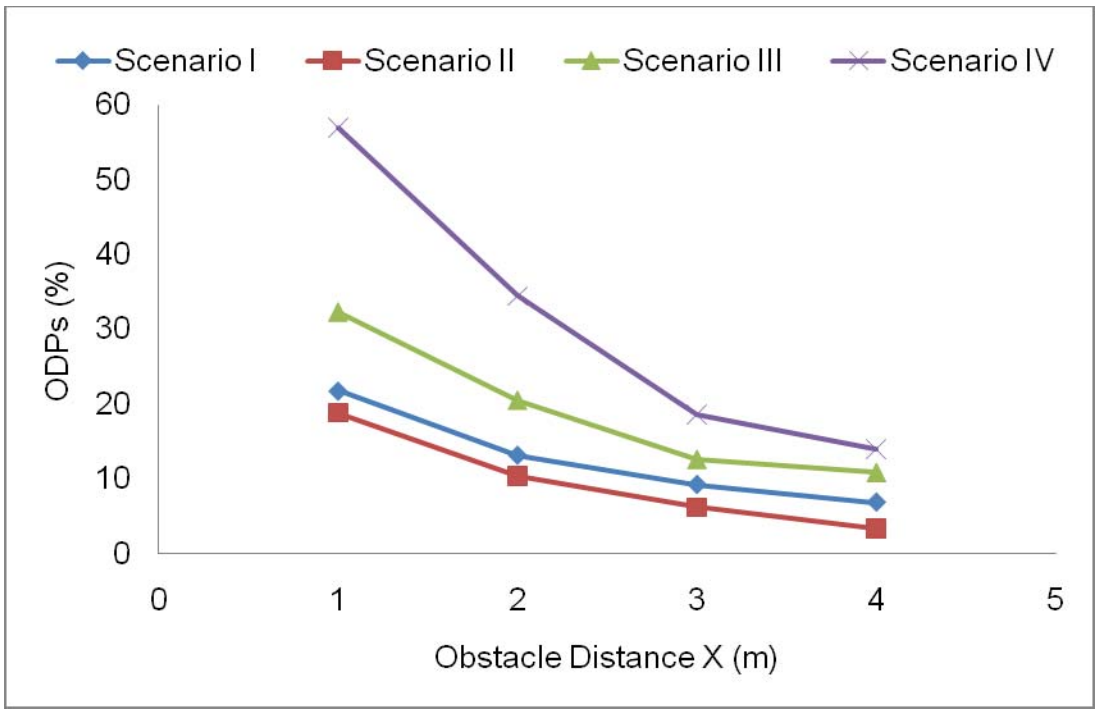

Figure 8. Effect of obstacle distance X on % of obstacle data points

In all scenarios, as the obstacle distance X increased from 1 to 4 m the percent of ODPs recorded decreased (fig.8). The percent of ODPs obtained in scenario IV was greater at all barrel distances of X because of the presence of three barrels in the field of view of the sensor array. Scenario 3 had the next highest percent of ODPs at all distances of X as both the RSA and LSA detected the barrel located straight ahead in line with the sensor array. The percent of ODPs obtained in scenario 1 and scenario 2 at all distances of X were less than the percent of ODPs recorded in scenario 3 and scenario 4 because in the first two scenarios most of the scanning by the IR sensor array detected no obstacles except for a single barrel present in one of the sensing planes. Further, it was observed that the percent of ODPs obtained for the LSA in scenario I was higher at all distances of X relative to the percent of ODPs obtained for the RSA in scenario II. This difference could be explained by the presence of undesirable data in between the barrel patterns (fig.5). The count of the ODPs with distance magnitude less than 4.5 m was increased due to the sensing of some unknown objects by the LSA causing the percent of ODPs recorded in scenario 1 to be higher than the percent of ODPs recorded in scenario 2.

Conclusions

The developed oscillating IR sensor array with a field view of 200^0 was able to detect the barrels in all four scenarios. The percent of ODPs recorded by the IR sensor array was the highest for scenario IV where the obstacle distance X was 1 m. A sensing range of 1 to 5.5 m, a field of view of 200^0, low computing power and low cost allows it to be a potential obstacle detection aid for UAgV's. Although the sensor array performed well under given test conditions, the response of the sensor array needs to be evaluated at different operating speeds and different obstacles. Future research will also involve utilizing the developed IR sensor array for obstacle avoidance.

References

1. Borenstein, J. and Koren, Y. 1998. Obstacle avoidance with ultrasonic sensors. IEEE Journal of Robotics and Automation, vol. 4, no. 2, 213-218

2. Gray, K. 2002. Obstacle detection sensor technology. Proceedings of Automation Technology for Off-Road Equipment, pp.442-450, Chicago, Illinois, USA

3. Matthies, L., C. Bergh, A. Castano, J. Masedo, and R. Manduchi. Obstacle detection in foliage with ladar and radar. In the proceedings of ISSR 2003, pp. 291-300, Siena, Italy

4. Wei, J., F.Rovira-Mas, J.F.Reid and S.Han. Obstacle detection using stereo vision to enhance safety of autonomous machines. 2005. Transactions of ASAE. Vol. 48(6): 2389−2397